PACS 81.40.-z

Effect of hydrogen on microstructure of α-Titanium alloys deformed at 600°C

M. A. Murzinova

mma@imsp.ru

Institute for Metals Superplasticity Problems, RAS, 39 Khalturin St., 450001, Ufa, Russia

Data on microstructural parameters of commercial pure titanium and α-titanium alloy Ti-5Al-2.5Sn with various hydrogen content strained at 600 °C are represented. Technique of electron backscattering diffraction was applied for quantitative analysis of the microstructure. Obtained results and literature data were used to analyze the relationships between flow stress and the mean grain size in deformed alloys. It was shown that continuous dynamic recrystallization occurred in the Ti-5Al-2.5Sn alloy at deformation conditions used in the present study. In this case the effect of hydrogen on the flow stress and microstructure of deformed alloy was very weak. Under the same deformation conditions, the dynamic recrystallization in commercial pure titanium took place in accordance with both discontinuous and continuous mechanisms. At that the hydrogen dissolved in the α-phase led to decrease in flow stress and to refinement of recrystallized α-grains.

Keywords: titanium alloys, hydrogen, deformation, recrystallization.

1. Introduction

Numerous studies of hydrogen interaction with titanium alloys showed that hydrogen may be considered not only as an impurity but also as temporary[1] β-stabilizing alloying element to improve workability: (hot/warm working, machining, fusion welding, diffusion bonding, *etc*) and also to modify their microstructure [1—8]. In most cases, the beneficial effects mentioned above are explained by hydrogen-induced changes of the phase composition of the alloys [2—9].

At the same time, in hydrogenated titanium alloys the change of chemical composition of α- and β-solid solutions occurs, that affects on their own properties and structure modification during deformation and thermal treatment in a two-phase (α+β) — field and in the single-phase regions. For instance, it was shown that with increase in the concentration of dissolved hydrogen:

— grain growth rate decreased under annealing in α- and β- single-phase fields [7,10];

— the flow stresses of the β-phase in commercially pure titanium (CP Ti) and multi-component titanium alloys increased [3—6,9];

— on the contrary, the flow stresses of the α-phase of CP Ti decreased, but appreciable hydrogen effect on flow stresses of α-titanium alloy VT5–1 (Ti-5Al-2.5Sn) was not revealed [6, 9,10].

Hydrogen is the β-stabilizing element in titanium and its solubility in the β-phase amounts to tens of atomic percents [1,11]. Hydrogen leads to decrease in the temperature of transition to single β-phase field by hundreds of degrees [6, 11]. Therefore hydrogenated titanium alloys are treated in a single β-phase field and data on the properties and structure modification after such treatment are published quite a few and summarized in [3—6].

The solubility of hydrogen in the α-phase of titanium alloys does not exceed 8 at% and it decreases rapidly at temperatures either below 300 °C or above 750 °C [6,9,11]. So, it is a problem to perform treatment in such a narrow temperature-concentration α-phase field. In this regard, study of the effect of hydrogen on the flow stress and microstructure modification of titanium alloys deformed/annealed in single-phase α-region are limited, and their results are ambiguous [9, 10,12,13].

The objective of the present study is examination of the microstructure of CP titanium and VT5–1 alloy in initial and hydrogenated conditions, subjected to deformation in the single α-phase field and to compare the obtained data with previously published.

2. Experimental

Hot-rolled rods of CP Ti with chemical composition Ti-0.32Al-0.1Fe-0.07Si-0.05C-0.035N-0.1O-0.002H (wt%) and α-titanium alloy VT5–1 with chemical composition Ti-5.4Al-2.8Sn-0.03Fe-0.01Zr-0.01Si-0.03C-0.01N-0.11O-0.002H (wt%) were used as a starting materials. The hydrogen concentration in these base alloys was 0.002 wt% that corresponded to 0.1 at%. Cylindrical samples with the length-to-diameter ratio 1.5 were cut from the rods and annealed in vacuum at temperatures of the single β-phase field. Then some of them were soaked in a pure hydrogen atmosphere at 700 °C. The

[1] The reaction of hydrogen with titanium is reversible due to a positive enthalpy of solution in titanium [1]. Therefore hydrogen dissolved in titanium may be easily removed by vacuum annealing.

hydrogen levels were determined by weighing the samples before and after hydrogenation to the nearest 5×10^{-5}g. After such treatment, samples of CP Ti with hydrogen content of 5.3 at% and samples of the VT5–1 alloy with hydrogen content of 5.8 at% were obtained and denoted as CP Ti-5H and VT5-1-6H, correspondingly.

Coarse-grained lamellar-type microstructure was observed in all samples after performed treatment. The size of α-colonies was 300 – 500 μm and the thickness of α-lamellae was 5–15 μm.

All samples were subjected to deformation processing by the multistep isothermal forging in the single α-phase field at 600 ^{0}C with a total strain of about 5.

Microstructure of the forged samples was studied in their cross sections by electron backscatter diffraction (EBSD) technique. EBSD analyses was conducted using Mira 3 Tescan scanning electron microscope equipped with Oxford Instruments HKL Channel 5 software. Four or five blindly selected and widely separated fields were mapped to obtain a reasonable average for each specimen (scanned area of each map was 225 μm^2, scan step was 0.1 μm). Grain-boundary misorientations below 2° were excluded from the data analysis [14]. A boundary misorientation of 15° was used to define high-angle boundaries (HABs).

The value of equivalent diameter of grain was taken as a characteristic of grain size. Statistical data analisys was carried out in accordance with recommendations [15,16]. The relative accuracy of the measurements was less than 10% for VT5–1 and VT5-1-6H alloys and achieved 25 and 17% for CP Ti and CP Ti-5H alloys, respectively, for confidence interval of 95%.

3. Results and Discussion

Maps of microstructure and grain size distributions in the investigated alloys are shown in Fig.1a-e. During deformation at 600 ^{0}C, the initial lamellar microstructure was transformed to fine-grained one in all cases. The shape of grains was close to equiaxed, mean value of aspect ratio of the grains was less than 1.8, and the mean sizes of grains were by 5—10 times less than the thickness of initial α-lamellae. Consequently, dynamic recrystallization (DRX) occurred during the deformation.

Microstructure with the largest sizes of DRX α-grains is observed in CP Ti. It can be seen that, the grain size distribution is rather spreaded, so its maximum is can be hardly defined (Fig.1e). The quantity of grains with sizes from 1 to 3 μm is about the same, but number of the fine grains is larger than the coarse ones. As a result, the mean grain size is 1.6 μm. Microstructure of the alloy CP Ti-5H looks visually finer in comparison with the CP Ti (Fig.1b), but the mean size of DRX α-grains is 1.1 μm that is slightly less than in CP Ti taking into account the dispersion of data. The grain size distribution remains widely spreaded, but its maximum becomes more pronounced, and the number of fine grains (with the sizes less than 2 μm) is noticeably larger than that in the CP Ti (Fig.1e).

Microstructure of the VT5–1 and VT5-1-6H alloys is more homogeneous and finer (Fig.1c,d) in comparison with structure of CP Ti and CP Ti-5H alloys. The mean grain sizes are 0.8 and 0.7 μm in VT5–1 and VT5-1-6H alloys, respectively, that is the same within the experimental accuracy. The distribution of grain sizes is nearly lognormal (Fig.1e).

Deformation-induced LABs are observed inside the grains in all compositions. The mean sizes of grains and subgrains are close in each alloy. The misorientation angles of the most LABs are 5—12 degrees, therefore, these may be permanent interfaces [14,19]. As an example, typical point-to-point misorientation profile measured along the line AB marked in Fig.1b is shown in Fig.1f. Moreover, the LABs contains segments with misorientation higher than 15° and thus, «dangling» HABs are observed in the EBSD maps (see outlined areas in Fig.1a-d).

The represented data are qualitatively consistent with the results of [10]. As well as after deformation at higher temperatures, the presence of dissolved hydrogen does not affect the mean size of the DRX α-grains in the VT5–1 alloy and results in a decrease in the mean DRX α-grain size in CP Ti.

It is known [17—20] that the mean size of grains/subgrains, which form during hot/warm deformation, obeys a power-law of the steady-state flow stress (σ_{ss}) The empirical relationship can be expressed as [18—20], $\sigma_{ss}/G \propto KD^{-N}$ where G is the shear modulus of material, K is a constant and N is the grain size exponent. The value of N is 0.7—1, if dynamic recovery or discontinuous dynamic recrystallization (DDRX) occurs [17—26] and N is less than 0.5, if continuous dynamic recrystallization (CDRX) takes place [21—26]. The relationship between mean size of DRX α-grains and steady-state flow stress normalized by shear modulus for α-titanium alloys are shown in Fig.2. Shear modules at different temperatures were obtained from Ref. [12,27]. Data for CP Ti deformed in a wide temperature interval were taken from [23], some points for CP Ti and VT5–1 in initial and hydrogenated conditions were taken from [10], and the data obtained in the present work are plotted with larger symbols.

The authors [23—26] noted that bilinear relationship (like for CP Ti) reflects the change in the structural mechanisms responsible for DRX grain development under different processing conditions. The change in the mechanism of DRX from discontinuous to continuous one was observed at the stress level of about 7×10^{-3}G for CP Ti at deformation temperature T_d=650 ^{0}C and strain rate $e'=10^{-3}s^{-1}$ [23] (Fig.2). In this experiment both CP Ti and CP Ti-5H alloys showed close stresses at T_d=600 ^{0}C and $e'=5\times10^{-4}s^{-1}$. Therefore both mechanisms of DRX could operate in these cases, that confirmed by the results of the structural observations. Indeed, the wide variation in grain size (Fig.1e) is typical for the structure obtained after DDRX at $T_d\geq0.5T_m$ (T_m is the melting temperature) [17,19], when migration of HABs plays an important role in the structure evolution. In contrast, the presence of arrays of the LABs with relatively large misorientation angles, and «dangling» HABs (Fig.1a,b,f), the absence of clear difference in grain and subgrain sizes are typical for process of CDRX [24—26]. Hydrogen, dissolved in CP Ti, retarded the migration of α/α HABs [10]. Probably, this might lead to an increase in

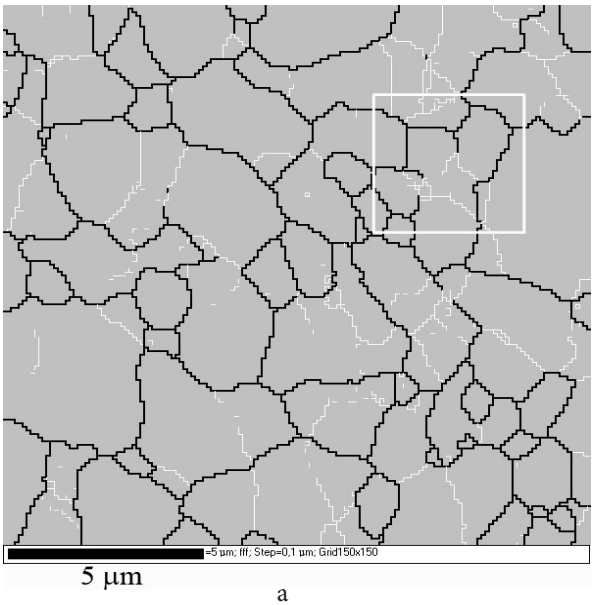

a

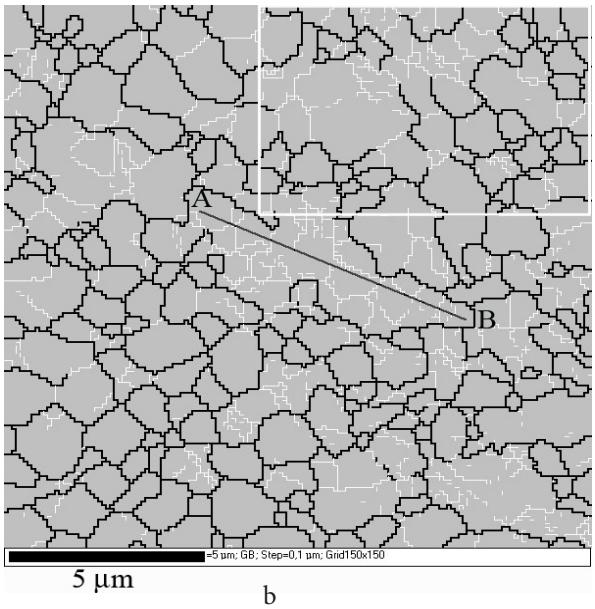

b

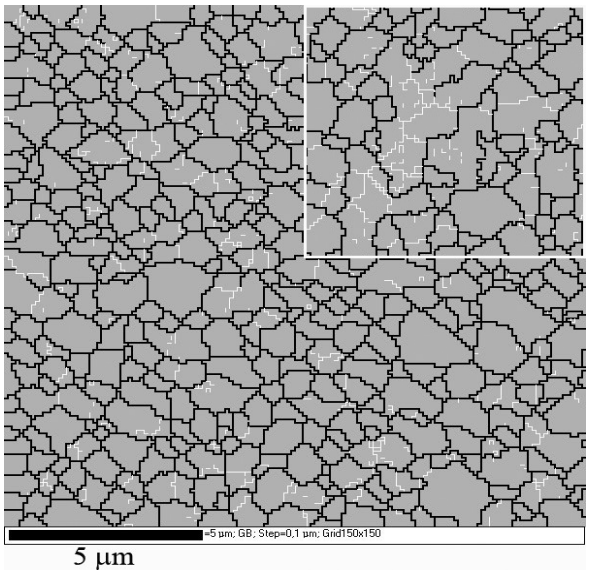

c

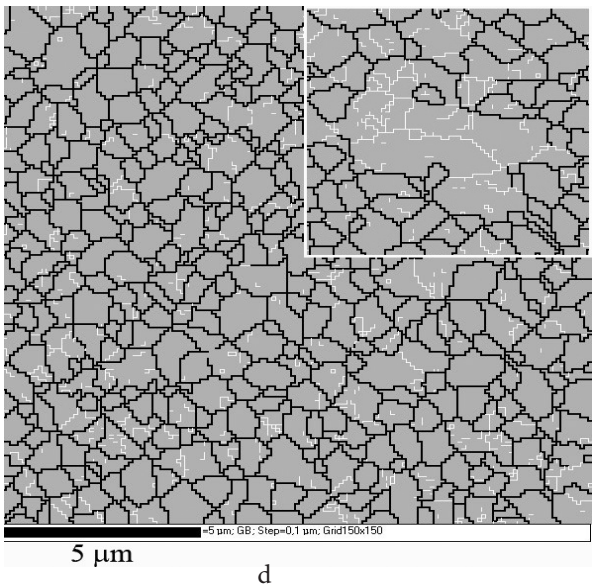

d

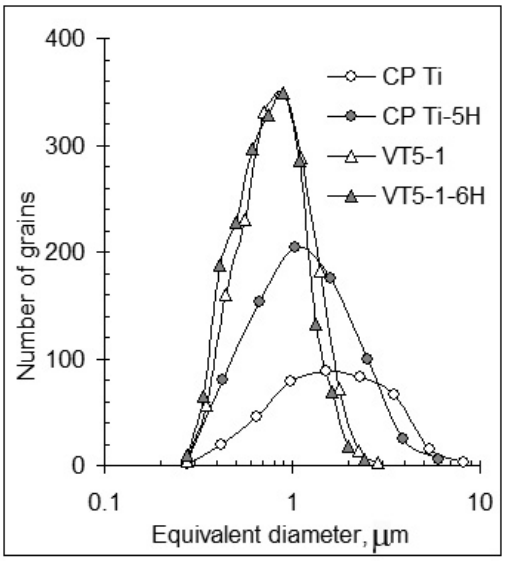

e

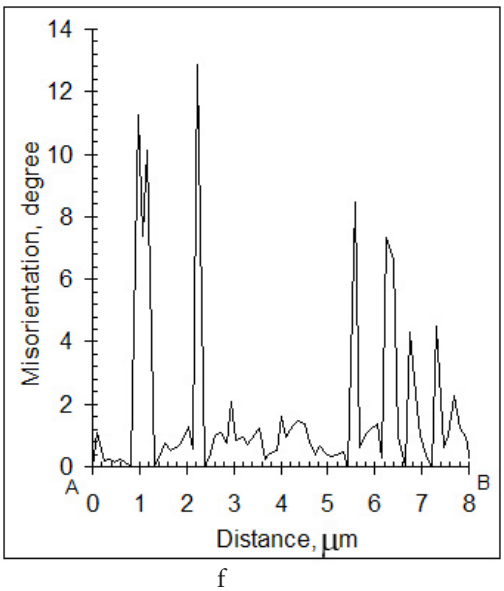

f

Fig. 1. Microstructure maps of CP Ti (a), CP Ti-5H (b), VT5–1 (c), VT5-1-6H (d) deformed at 600 ^{0}C, grain size distributions per surface area 1000 μm^2 in these alloys (e), point-to-point misorientation profile measured along the line AB marked in Fig.1b (f).

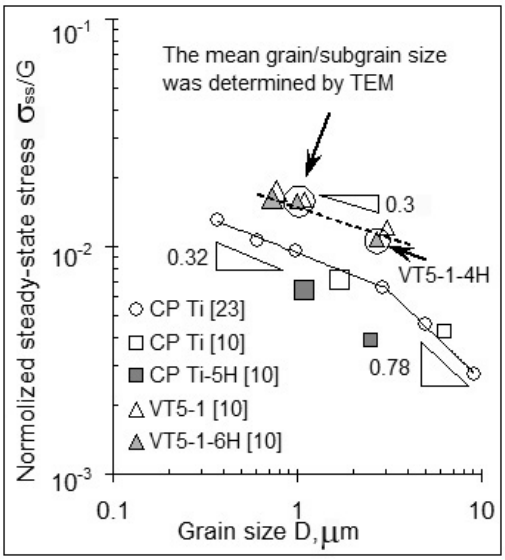

Fig. 2. The relationship between DRX α-grain size and steady-state flow stress normalized by shear modulus for α-titanium alloys.

the contribution of continuous processes in the formation of DRX α-grains in hydrogenated CP Ti at T_d=600^{0}C.

Most likely CDRX occurred during deformation of the VT5–1 and VT5-1-6H alloys at studied conditions of deformation. Indeed, structural features described above and values of the grain size exponent N close to 0.3, (Fig.2) are typical for CDRX [21—26]. If the migration of HABs was inhibited during deformation, the effect of hydrogen on the mean size of DRX α-grain was not revealed. Nevertheless, such explanation cannot exclude an assumption that the influence of hydrogen is imperceptible due to presence of aluminum and tin in α-phase of the VT5–1 alloy. To verify this assumption it would be interesting to compare the structure and properties of VT5–1 and VT5-1-5H alloys deformed in single α-phase field at higher temperatures. But, the hydrogen solubility decreases rapidly at temperatures above 750 ^{0}C, and it is impossible to perform such an experiment.

4. Conclusion

Microstructure of deformed CP Ti and VT5–1 alloys with conventional hydrogen content (0.1 at.%) and hydrogen content close to the limit of solubility at deformation temperature 600 ^{0}C (~0.45T_m) were examined with EBSD technique. Effect of hydrogen on α-grains refinement was observed in CP Ti and was not revealed in VT5–1 alloy. It was shown that CDRX takes place in the base and hydrogenated VT5–1 alloy and both DDRX and CDRX can operate in the base and hydrogenated CP Ti under the same deformation conditions. Thus, the favorable effect of hydrogen on the α-grain refinement may be explained in terms of retarding/inhibition the migration of HABs during DRX.

The author would like to thank Dr D. D. Afonichev for his kind help in preparation of the samples and Dr. O. Sh. Sitdikov for the fruitful discussions. The work was partially supported by the Russian Foundation for Basic Research (under research projects 09-02-92666-IND_a and 11-08-00404-a).

References

1. Hidrogen in Metalas III. Ed. by H. Wipf, Springer. (1997) 340 p.
2. W. R. Kerr, Metall. Mater. Trans. **A16**, 1077 (1985).
3. O. N. Senkov, J. J. Jonas, F. H. Froes. JOM. **48** (7), 42 (1996).
4. A. A. Ilyin, B. A. Kolachev, V. K. Nosov, in: V. Goltsov (Ed.), Progress in Hydrogen Treatment of Materials, Donetsk — Coral Gables: Kassiopeya LTD. (2001) p. 299.
5. O. N. Senkov, F. H. Froes. Hydrogen Energy. **24**, 565 (1999).
6. A. A. Ilyin, B. A. Kolachev, V. K. Nosov, A. M. Mamonov. Hydrogen processing of titanium alloys. Ed.by A. A. Ilyin, Moscow, MISIS. (2002) 392 p. (in Russian)
7. M. A. Murzinova, G. A. Salishchev, D. D. Afonichev. Int. J. Hydrogen Energy. **27**, 775 (2002).
8. M. A. Murzinova, G. A. Salishchev, D. D. Afonichev. Phys. Met. Metallogr. **104**(2), 195 (2007).
9. O. N. Senkov, J. J. Jonas. Metall. Mater. Trans. **A27** (7), 1869 (1996).
10. M. A. Murzinova, G. A. Salishchev, D. D. Afonichev. Mater. Sci. Forum. **467—470**, 1223 (2004).
11. O. N. Senkov, J. J. Jonas. Metall. Mater. Trans. **A27**(7), 1877 (1996).
12. O. N. Senkov, M. Dubois, J. J. Jonas. Metall. Mater. Trans. **A27**(12), 3963 (1996).
13. H. Okamoto, in ASM Handbook, Volume 3. Alloy Phase Diagrams. 1-st Printing, E-Publishing, ASM International. (1992) p.989.
14. F. J. Humphreys. J. Mater. Sci. **36**, 3833 (2001).
15. ASTM E112–10.
16. M. A. Shtremel. Strength of alloys. Part 1. Moscow, MISIS (1999) 384 p. (in Russian)
17. T. Sakai, J. J. Jonas. Acta Metall. **32**(2), 189 (1984).
18. B. Derby. Acta Metall. Mater. **39**(5), 955 (1991).
19. F. J. Humphreys and M. Hatherly. Recrystallization and Related Annealing Phenomena, 2nd ed. Elsevier Ltd. (2004) 628 p.
20. H. J. McQueen, Metall. Sci, & Technology. **28—1**, 12 (2010).
21. H. Beladi, P. Cizek, P. D. Hodgson. Metall. Mater. Trans. **40 A**, 1175 (2009).
22. A. Galiyev, R. Kaibyshev, G. Gottstein. Acta Mater. **49**, 1199 (2001).
23. S. V. Zherebtsov, G. A. Salishchev, R. M. Galeyev. Defect and Diffusion Forum. **208—209**, 237 (2002).
24. A. Belyakov, T. Sakai, H. Miura, K. Tsuzaki. Philos. Mag. **A81**, 2629 (2001).
25. A. Belyakov, K. Tsuzaki, H. Miura, T. Sakai. Acta Mater. **51**, 847 (2003).
26. N. Dudova, A. Belyakov, T. Sakai, R. Kaibyshe. Acta Mater. **58**, 3624 (2010).
27. Materials in mechanical engineering. Vol. 1. Nonferrous metals and alloys. Ed. by I. V. Kudrayvcev, L. P. Luzhnikov. Handbook in 5 volumes. Moscow, Mechanical engineering (1967) 304 p. (in Russian)